

Robust Generation Dispatch with Strategic Renewable Power Curtailment and Decision-Dependent Uncertainty

Yue Chen, *Member, IEEE* and Wei Wei, *Senior Member, IEEE*

Abstract—As renewable energy sources replace traditional power sources (such as thermal generators), uncertainty grows while there are fewer controllable units. To reduce operational risks and avoid frequent real-time emergency controls, a preparatory schedule of renewable generation curtailment is required. This paper proposes a novel two-stage robust generation dispatch (RGD) model, where the curtailment strategy is optimized in the pre-dispatch stage. The curtailment strategy will then influence the real-time renewable power output, resulting in a decision-dependent uncertainty (DDU) set. In the re-dispatch stage, the controllable units adjust their outputs within the reserve capacities to maintain power balancing. To overcome the difficulty in solving the RGD with DDU, an adaptive column-and-constraint generation (AC&CG) algorithm is developed. We prove that the proposed algorithm can generate the optimal strategy in finite iterations. Numerical examples validate the practicability and scalability of the proposed model and algorithm.

Index Terms—generation dispatch, decision-dependent uncertainty, robust optimization, curtailment, adaptive C&CG

NOMENCLATURE

A. Abbreviations

RG	Renewable generator.
RGD	Robust generation dispatch.
C&CG	Column-and-constraint generation.
DDU	Decision-dependent uncertainty.
SO	Stochastic optimization.
RO	Robust optimization.
DRO	Distributionally robust optimization.

B. Indices, Sets, and Functions

$\mathcal{W}(\xi)$	Decision-dependent uncertainty set.
$Q(p, r^\pm, w)$	The optimal objective value of the re-dispatch problem when the RG output is w .
$S(x, \xi)$	The optimal objective value of the inner “max-min” problem given the first-stage decisions x, ξ .
\mathcal{AC}_n	Set of active constraints in iteration n .

C. Parameters

N_g	Number of thermal units.
N_w	Number of renewable generators.
N_l	Number of loads.
N_k	Number of transmission lines.
T	Number of dispatch periods.
Γ_S, Γ_T	Spatial/Temporal uncertainty budget.
W_{jt}^e	Forecast output of RG j in period t .
W_{jt}^u, W_{jt}^l	Upper/Lower bound of the confidence interval of power output of RG j in period t .
α_i	Running cost coefficient of thermal unit i .
β_i^\pm	Upward/Downward reserve cost coefficient of thermal unit i .
γ_j	Curtailment cost coefficient of RG j .
P_i^u, P_i^l	Maximum/Minimum output of thermal unit i .
$\mathcal{R}_i^d, \mathcal{R}_i^u$	Ramping limit of thermal unit i .
R_i^\pm	Maximum/Minimum reserve of thermal unit i .
\mathcal{D}_{lt}	Demand of load l in period t .
F_k	Capacity of transmission line k .
$\pi_{ik}, \pi_{jk}, \pi_{lk}$	Line flow distribution factors.
d_i^\pm	Upward/Downward regulation cost coefficient of thermal unit i .

D. Decision Variables

ξ_{jt}	Curtailment of RG j in period t .
\hat{w}_{jt}	Output before curtailment of RG j in period t .
w_{jt}	Output after curtailment of RG j in period t .
w_{jt}^u, w_{jt}^l	The amount by which the power output of RG j deviates upward/downward from the forecast.
z_{jt}, \hat{z}_{jt}	Binary variables for linearization.
p_{it}	Contemporary output of thermal unit i in t .
r_{it}^\pm	Reserve capacity of thermal unit i in period t .
p_{it}^\pm	Incremental outputs of thermal unit i in t .

I. INTRODUCTION

ONE effective way to mitigate global warming is the massive deployment of renewable energy. In 2020, wind power with an incremental capacity of 93GW was installed, boosting the total global capacity to 743 GW [1]. Despite a decrease in energy consumption due to COVID-19 in 2020, the global cumulative solar capacity increased by 22%, establishing a new milestone for the solar sector [2]. At the same time, increasing renewable energy penetration poses a significant challenge to power system operation due to its intermittent, volatile, and uncertain characteristics. Generation

Y. Chen is with the Department of Mechanical and Automation Engineering, the Chinese University of Hong Kong, Hong Kong SAR (email: yuechen@mae.cuhk.edu.hk)

W. Wei is with the the State Key Laboratory of Power Systems, Department of Electrical Engineering, Tsinghua University, Beijing 100084 China. (wei-wei04@mails.tsinghua.edu.cn)

This work has been submitted to the IEEE for possible publication. Copyright may be transferred without notice, after which this version may no longer be accessible.

dispatch (a generalization of economic dispatch) is widely used to deal with uncertainties by altering the real-time output of controllable generators within reserve capacity to hedge against renewable power output fluctuations [3].

Traditional generation dispatch models under uncertainty were based on stochastic optimization (SO) [4], [5], robust optimization (RO) [3], [6], and distributionally robust optimization (DRO) [7], [8]. Stochastic optimization aims to minimize the expected cost or to meet certain chance constraints based on the assumption that the renewable generator (RG) output follows a known probability distribution. However, in practice, though we can obtain a rough histogram via historical data, it is hard to procure the exact probability distribution. Deviation from the real distribution may result in sub-optimal or even infeasible solutions. In contrast, RO considers all possible realizations of RG output in a prespecified uncertainty set and comes up with the dispatch strategy that minimizes the cost under the worst-case scenario. Various effective algorithms, such as Bender's decomposition [9] and column-and-constraint generation (C&CG) [10], were put forward to get the robust optimal solution efficiently. DRO is in-between SO and RO. Instead of using an uncertainty set, it describes the RG output by all possible probability distributions with the same mean and variance recovered from the historical data. Though DRO is less conservative than RO, it is time-consuming since it involves solving a semi-definite programming [8]. Therefore, this paper adopts the robust generation dispatch (RGD) model.

In most existing literature, the uncertainty set in a RGD model is determined based on all available renewable generation, implicitly assuming that 100% of renewable generation can be used without curtailment. However, as renewable energy sources replace conventional power sources (e.g., thermal generators), uncertainty increases while there are fewer controllable units. As a result, curtailment of renewable energy is inevitable to maintain system security [11]. References [12] and [13] developed two-stage unit commitment models taking into account the wind power curtailment. However, the curtailment only happens in real-time without preparatory schedules, which may lead to a large number of RGs being shut down in real-time, causing operational risks such as instability or oscillation. Reference [14] emphasized the need of considering curtailment in the pre-dispatch stage so that we can have a relatively long time to make adjustments.

When the curtailment of renewable energy is incorporated in the pre-dispatch stage, the variation range of real-time RG output will be influenced. Therefore, distinct from the uncertainty sets in traditional robust optimization models that are pre-specified, the uncertainty set in our model depends on the first-stage decision. *Decision-dependent uncertainty* (DDU) has captured great attention in recent years and most existing works deal with DDU via stochastic programming [15], [16]. As for robust optimization, reference [17] provided a reformulation method to solve the *static* robust model with DDU where only "here-and-now" variables were included and the size of uncertainty set merely depends on binary variables. Another robust counterpart model was established in [18] with a more general set. In practice, *adjustable* robust optimization is more commonly used since it can describe

the adjustment behaviors after the realization of the uncertain factors. The solution of adjustable robust optimization with DDU can be estimated via a K-adaptability approximation based algorithm [19]. Multi-parametric programming [20] and modified Bender's decomposition [21] were deployed to offer an exact solution. However, they are either time-consuming with a growing number of participants or concentrated on the linear DDU set. In general, robust optimization with DDU is an important albeit challenging problem due to its computational intractability.

This paper proposes a robust generation dispatch model considering curtailment in the pre-dispatch stage. An adaptive C&CG algorithm is developed to solve the problem efficiently in finite iterations. Our main contributions are two-fold:

1) **Robust generation dispatch model with DDU.** A novel RGD model considering renewable energy curtailment in the pre-dispatch stage is proposed. Curtailment is defined as the upper limit of actual RG output, which is co-optimized with the contemporary output and reserve capacity of thermal generators. This enables a preparatory schedule of curtailment and avoids frequent real-time emergency control, which is more practical. Distinct from the traditional RGD models, the uncertain RG output is influenced by the curtailment strategy, and thus, is decision-dependent. The real-time RG output is the minimum of the actual RG output and the curtailment strategy. We further linearize this nonlinear relationship, turning the uncertainty set into a mixed-integer linear DDU set.

2) **Adaptive C&CG Algorithm.** With decision-dependent uncertainty, the traditional robust optimization algorithms cannot be applied since the previously selected scenario may be outside of the uncertainty set as the pre-dispatch strategy changes. In this paper, an adaptive C&CG algorithm is developed. We add the active constraints under the worst-case scenario rather than the worst-case scenario itself to the master problem in each iteration. Two types of degeneracy that may occur during active constraints identification are addressed. When the pre-dispatch strategy changes, the scenario generated by the active constraints remains a vertex of the new uncertainty set. We proved that our algorithm can generate the robust optimal solution in finite iterations. Case studies show that our algorithm can greatly reduce the computational time compared with the nested C&CG (which may still be applied but without the theoretical guarantee of finite-step-ending).

The rest of this paper is organized as follows. Section II introduces the decision-dependent uncertainty set and the robust generation dispatch model. An adaptive C&CG algorithm is developed in Section III to solve the problem. Case studies are given in Section IV with conclusions in Section V.

II. MATHEMATICAL FORMULATION

We consider a two-stage generation dispatch problem for a system with N_g thermal generators, N_w renewable generators (RGs), and T dispatch periods. In the first-stage (*pre-dispatch stage*), the contemporary output and reserve capacity of thermal generators are determined based on the RG forecast outputs. Moreover, the curtailment of RGs is also considered to adapt to the increasing fluctuation due to higher renewable

energy penetration. In the second-stage (*re-dispatch stage*), the thermal generators adjust their outputs within their reserve capacities to maintain real-time power balancing. In the following, we first introduce the RG output uncertainty set, which is influenced by the first-stage curtailment strategy. Then the robust generation dispatch model with DDU is proposed.

A. Decision-dependent uncertainty set

In this paper, the curtailment of RGs is considered in the first-stage to avoid frequent calls of emergency control in real-time. The curtailment is defined as an upper limit of the actual RG output, denoted as $\xi_{jt}, \forall j, \forall t$. Denote the actual output and output after curtailment of RG j in period t as \hat{w}_{jt} and w_{jt} , respectively. Then, the uncertainty set $\mathcal{W}(\xi)$ is given as follows, depending on the curtailment strategy ξ .

$$\mathcal{W}(\xi) = \left\{ w \left| \begin{array}{l} w_{jt} = \min\{\hat{w}_{jt}, \xi_{jt}\}, \forall j, \forall t \\ \hat{w}_{jt} = W_{jt}^e + w_{jt}^u - w_{jt}^l, \forall j, \forall t \\ 0 \leq w_{jt}^l, w_{jt}^u \leq W_{jt}^h, \forall j, \forall t \\ w_{jt}^l w_{jt}^u = 0, \forall j, \forall t \\ \sum_{j=1}^{N_w} \frac{w_{jt}^l + w_{jt}^u}{W_{jt}^h} \leq \Gamma_S, \forall t \\ \sum_{t=1}^T \frac{w_{jt}^l + w_{jt}^u}{W_{jt}^h} \leq \Gamma_T, \forall j \end{array} \right. \right\} \quad (1)$$

where $W_{jt}^e = (W_{jt}^l + W_{jt}^u)/2$, $W_{jt}^h = (W_{jt}^u - W_{jt}^l)/2, \forall j, \forall t$.

The RG output after curtailment is the minimum of the actual RG output and the upper limit, as in the first constraint. The remaining constraints limit the deviation of the actual RG output. To be specific, the actual RG output fluctuates within a range $[W_{jt}^l, W_{jt}^u]$ whose mean is the forecast value W_{jt}^e . When the RG output is higher than its forecast, $w_{jt}^u > 0, w_{jt}^l = 0$; otherwise, $w_{jt}^u = 0, w_{jt}^l > 0$. To avoid over-conservativeness of the model, uncertainty budgets Γ_S and Γ_T are added to restrain the spatial and temporal deviations from the prediction.

The above uncertainty set involves nonlinear constraints $w_{jt} = \min\{\hat{w}_{jt}, \xi_{jt}\}, \forall j, \forall t$, each of which can be linearized by introducing a binary variable as below

$$w_{jt} \leq \hat{w}_{jt}, w_{jt} \leq \xi_{jt} \quad (2a)$$

$$\hat{w}_{jt} - (W_{jt}^u - W_{jt}^l)(1 - z_{jt}) \leq w_{jt} \quad (2b)$$

$$\xi_{jt} - (\xi_{jt} - W_{jt}^l)z_{jt} \leq w_{jt} \quad (2c)$$

$$z_{jt} \in \{0, 1\} \quad (2d)$$

when $z_{jt} = 0$, constraints (2a) and (2c) lead to $w_{jt} = \xi_{jt} \leq \hat{w}_{jt}$, while (2b) becomes $\hat{w}_{jt} - w_{jt} \leq W_{jt}^u - W_{jt}^l$ which is always satisfied. In this case, there is surplus RG output and curtailment is executed. When $z_{jt} = 1$, constraints (2a) and (2b) lead to $w_{jt} = \hat{w}_{jt} \leq \xi_{jt}$, while (2c) becomes $w_{jt} \geq W_{jt}^l$ which is always satisfied. Thus, no RG output is curtailed. The other nonlinear constraint $w_{jt}^l w_{jt}^u = 0$ can be linearized as

$$0 \leq w_{jt}^l \leq M\hat{z}_{jt}, 0 \leq w_{jt}^u \leq M(1 - \hat{z}_{jt}), \hat{z}_{jt} \in \{0, 1\} \quad (3)$$

where M is a large constant.

After the above transformation, the uncertainty set (2) consists of mixed-integer linear constraints. Moreover, it relies on the value of the first-stage curtailment strategy ξ , and thus, is

decision-dependent. Traditional algorithms for solving robust optimization with decision-independent uncertainty sets are the Bender's decomposition [9] and the C&CG algorithm [10]. They are guaranteed to converge in a finite number of steps since a different vertex of the uncertainty set is added to the master problem in each iteration, and the number of vertices is finite. However, with a decision-dependent uncertainty set, when the first-stage decision changes, the previously selected scenario may no longer be a vertex of the new uncertainty set. As a result, the traditional algorithms may fail to converge. In this paper, we develop an adaptive C&CG algorithm to address this issue, which will be explained in detail in Section III.

B. Robust generation dispatch model

The robust generation dispatch model considering curtailment of RGs is given below:¹

$$\min_{p, r^\pm, \xi} \sum_{t=1}^T \sum_{i=1}^{N_g} (\alpha_i p_{it} + \beta_i^+ r_{it}^+ + \beta_i^- r_{it}^-) + \sum_{t=1}^T \sum_{j=1}^{N_w} \gamma_j (W_{jt}^u - \xi_{jt})^2 + \max_{w \in \mathcal{W}(\xi)} Q(p, r^\pm, w) \quad (4a)$$

$$\text{s.t. } W_{jt}^l \leq \xi_{jt} \leq W_{jt}^u, \forall j \in [N_w], \forall t \in [T] \quad (4b)$$

$$P_i^l \leq p_{it} \leq P_i^u, \forall i \in [N_g], \forall t \in [T] \quad (4c)$$

$$-R_i^d \leq p_{it} - p_{i(t-1)} \leq R_i^u, \forall i \in [N_g], \forall t \in [T]/\{1\} \quad (4d)$$

$$P_i^l \leq p_{it} - r_{it}^-, p_{it} + r_{it}^+ \leq P_i^u, \forall i \in [N_g], \forall t \in [T] \quad (4e)$$

$$0 \leq r_{it}^- \leq R_i^-, 0 \leq r_{it}^+ \leq R_i^+, \forall i \in [N_g], \forall t \in [T] \quad (4f)$$

$$\sum_{j=1}^{N_w} W_{jt}^e + \sum_{i=1}^{N_g} p_{it} = \sum_{l=1}^{N_l} D_{lt}, \forall t \in [T] \quad (4g)$$

$$-F_k \leq \sum_{i=1}^{N_g} \pi_{ik} p_{it} + \sum_{j=1}^{N_w} \pi_{jk} W_{jt}^e$$

$$-\sum_{l=1}^{N_l} \pi_{lk} D_{lt} \leq F_k, \forall k \in [N_k], \forall t \in [T] \quad (4h)$$

The first-stage decisions, including the contemporary output $\{p_{it}, \forall i, \forall t\}$ and reserve capacity $\{r_{it}^\pm, \forall i, \forall t\}$ of thermal units, and the curtailment strategy $\{\xi_{jt}, \forall j, \forall t\}$, are made prior to the realization of uncertainty. The objective function (4a) minimizes the sum of generation cost, reserve cost, curtailment cost, and the re-dispatch cost under the worst-case scenario. The curtailment strategy is between the lower and upper bounds of the actual RG output as in constraint (4b). Constraints (4c), (4d), and (4f) represent the limits of generation capacity, ramping rate, and reserve capacity, respectively. The generation adequacy is ensured in (4e). Power balancing condition and power flow limits are given in (4g) and (4h), respectively. The term $Q(p, r^\pm, w)$ in (4a) is the re-dispatch cost when the RG output is w . Therefore, maximizing $Q(p, r^\pm, w)$ over all possible $w \in \mathcal{W}(\xi)$ gives the cost under the worst-case scenario. Here, $\mathcal{W}(\xi)$ is the decision-dependent uncertainty set (1). To be specific, $Q(p, r^\pm, w)$ is the optimal objective value of the second-stage re-dispatch problem:

$$\min_{p^\pm} \sum_{t=1}^T \sum_{i=1}^{N_g} (d_i^+ p_{it}^+ + d_i^- p_{it}^-) \quad (5a)$$

$$\text{s.t. } 0 \leq p_{it}^+ \leq r_{it}^+, 0 \leq p_{it}^- \leq r_{it}^-, \forall i \in [N_g], \forall t \in [T] \quad (5b)$$

¹[A] denotes all positive integers that do not exceed A.

$$\sum_{i=1}^{N_g} (p_{it} + p_{it}^+ - p_{it}^-) + \sum_{j=1}^{N_w} w_{jt} = \sum_{l=1}^{N_l} \mathcal{D}_{lt}, \quad \forall t \in [T] \quad (5c)$$

$$\begin{aligned} -F_k &\leq \sum_{i=1}^{N_g} \pi_{ik} (p_{it} + p_{it}^+ - p_{it}^-) + \sum_{j=1}^{N_w} \pi_{jk} w_{jt} \\ &\quad - \sum_{l=1}^{N_l} \pi_{lk} \mathcal{D}_{lt} \leq F_k, \quad \forall k \in [N_k], \quad \forall t \in [T] \end{aligned} \quad (5d)$$

The second-stage decisions, including the incremental outputs of thermal units $\{p_{it}^\pm, \forall i, \forall t\}$, are made after knowing the exact outputs of RGs. The objective function (5a) is to minimize the re-dispatch cost, i.e., the sum of up- and down-regulation costs. Constraint (5b) requires the incremental output of thermal unit be within its reserve capacity. Power balancing condition and power flow limits are (5c) and (5d).

C. Compact form

The aforementioned robust generation dispatch model with decision-dependent uncertainty can be written in the following compact form:

$$\min_{x \in \mathbb{X}, \xi \in \Xi} c^\top x + g(\xi) + \max_{w \in \mathcal{W}(\xi)} \min_{y \in \mathbb{F}(x, w)} d^\top y \quad (6)$$

and

$$\begin{aligned} \mathbb{X} &= \{x \in \mathbb{R}^{3N_g \times T} : Ax \geq b\} \\ \Xi &= \{\xi \in \mathbb{R}^{N_w \times T} : B\xi \leq e\} \\ \mathcal{W}(\xi) &= \{w \in \mathbb{R}^{N_w \times T} : Hw \leq C\hat{w} + F\xi + Gz + a, \\ &\quad \forall z \in \mathbb{Z}^{2N_w \times T}, \hat{w} \in \mathbb{R}^{3N_w \times T}\} \\ \mathbb{F}(x, w) &= \{y \in \mathbb{R}^{2N_g \times T} : Ey \leq f - Rw - Dx\} \end{aligned} \quad (7)$$

where $x := \{p_{it}, r_{it}^+, r_{it}^-, \forall i, \forall t\}$ and c is a collection of $\alpha_i, \beta_i^+, \beta_i^-, \forall i$. ξ is a collection of $\xi_{jt}, \forall j, \forall t$; $g(\xi) = (W^u - \xi)^\top \text{diag}(\gamma_1, \dots, \gamma_{N_w})(W^u - \xi)$. $w := \{w_{jt}, \forall j, \forall t\}$, $\hat{w} := \{\hat{w}_{jt}, w_{jt}^l, w_{jt}^u, \forall j, \forall t\}$, and z is a collection of the binary variables z_{jt} and \hat{z}_{jt} for all j, t . $y := \{p_{it}^+, p_{it}^-, \forall i, \forall t\}$; d is a collection of $d_i^+, d_i^-, \forall i$. $A, B, H, C, F, G, E, R, D$ and b, e, a, f are the coefficient matrices and vectors.

III. SOLUTION ALGORITHM

Different from the traditional robust optimization models [3], the uncertainty set in (6) is *decision-dependent*. The widely-used algorithms for solving the traditional robust optimizations may cause oscillation because the update of the first-stage decision keeps changing the shape as well as the extreme points of the uncertainty set. In this section, an adaptive C&CG algorithm is proposed to generate the optimal solution in a finite number of iterations.

A. Equivalent transformation

Given the first-stage decisions $x \in \mathbb{X}$ and $\xi \in \Xi$, the second-stage problem is a bilevel optimization:

$$S(x, \xi) := \max_{w \in \mathcal{W}(\xi)} \min_{y \in \mathbb{F}(x, w)} d^\top y \quad (8)$$

where $\mathbb{F}(x, w)$ is a polyhedral set while $\mathcal{W}(\xi)$ is bounded and consists of mixed-integer linear constraints depending on

the value of ξ in the first-stage. We first replace the inner minimization problem with its KKT condition and linearize the complementary and slackness condition in the form of $0 \leq x \perp y \geq 0$ using Big-M method [22]. Then the second-stage problem is equivalent to

$$\max_{w \in \mathcal{W}(\xi), y} d^\top y \quad (9a)$$

$$\text{s.t. } d + E^\top \mu = 0 \quad (9b)$$

$$0 \leq \mu \leq \hat{M} z_\mu \quad (9c)$$

$$0 \leq (-Ey + f - Rw - Dx) \leq \hat{M}(1 - z_\mu) \quad (9d)$$

$$z_\mu \in \{0, 1\}^{n_\mu} \quad (9e)$$

where n_μ is the number of constraints in (5), μ is the dual variable, and \hat{M} is a large enough constant. We denote the above optimization (9) as the subproblem **SP**.

Proposition 1. The optimal solution w^* of the subproblem **SP** will be reached at one of the extreme points of $\mathcal{W}(\xi)$.

Proof. Given x and ξ , the uncertainty set $\mathcal{W}(\xi)$ can be seen as the union of $2^{2N_w \times T}$ polytopes, each of which corresponds to a particular assignment to the set of binary variables $z \in \mathbb{Z}^{2N_w \times T}$, i.e., $\mathcal{W}(\xi) = \mathcal{W}^1(\xi) \cup \mathcal{W}^2(\xi) \cup \dots \cup \mathcal{W}^{2^{2N_w \times T}}(\xi)$. $Q(x, w) := \min_{y \in \mathbb{F}(x, w)} d^\top y$ is a quasiconvex function in w , so the optimal solution of $\max_{w \in \mathcal{W}(\xi)} Q(x, w)$ will be achieved at the extreme point of $\mathcal{W}(\xi)$ [23]. The argmin $_{w \in \mathcal{W}(\xi)} Q(x, w), \forall p \in [2^{2N_w \times T}]$ with the highest objective value is the optimal solution of (8), which is also an extreme point of $\mathcal{W}(\xi)$. \square

Suppose the optimal solution of the subproblem **SP** is (w^*, y^*) and the corresponding value of the second-stage binary variable is z^* . At the optimal point, the set of active and inactive constraints in $\mathcal{W}(\xi)$ are

$$H_{eq}w = C_{eq}\hat{w} + F_{eq}\xi + G_{eq}z + a_{eq} \quad (10)$$

$$H_{in}w < C_{in}\hat{w} + F_{in}\xi + G_{in}z + a_{in} \quad (11)$$

If we fix the value of z to z^* , then in non-degenerate cases, the matrix $[H_{eq}, -C_{eq}]$ is a $(4N_w \times T)$ -dimensional full rank matrix as the active constraints form a set of basis. For any given ξ , the value of (w, \hat{w}) can be uniquely determined by

$$\begin{bmatrix} w \\ \hat{w} \end{bmatrix} = [H_{eq}, -C_{eq}]^{-1} (F_{eq}\xi + G_{eq}z^* + a_{eq}) \quad (12)$$

However, in degenerate cases, it could be hard to recover w and \hat{w} using the active constraints. Methods to deal with this challenge are introduced in the following. Denote the set of active constraints we finally obtain in iteration n as \mathcal{AC}_n .

B. Model degeneracy

In general, two types of degeneracy may occur, i.e., primal degeneracy and dual degeneracy, which are illustrated in Fig. 1. Primal degeneracy is caused by weak redundant constraints. For example, in Fig. 1(a), constraints C1-C3 are all active at the optimal point so equation (10) is over-determined. In fact, constraint C3 is redundant: although C3 intersects the feasible region, removing C3 will not change the feasible region. The impact of primal degeneracy is manageable, because redundant

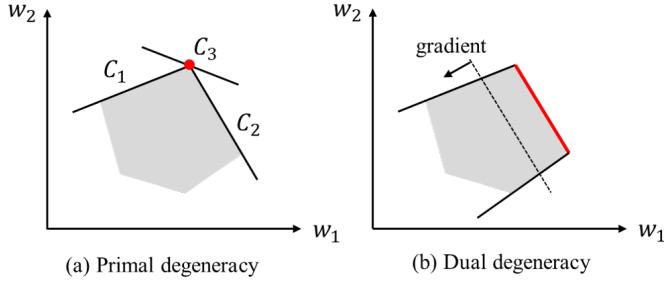


Fig. 1. Illustration of degenerate cases.

constraints in $\mathcal{W}(\xi)$ can be filtered before identifying the active constraints, and then $[H_{eq}, -C_{eq}]$ is invertible. The method for removing redundant constraints is given in Appendix A. In particular, we need to be careful about three cases:

- 1) If $w_{jt}^* = W_{jt}^u$: In this case, we must have $w_{jt}^* = \xi_{jt}$; otherwise, we have $w_{jt}^* = \hat{w}_{jt}^* \leq \xi_{jt} \leq W_{jt}^u$. Equality holds for all inequalities in the middle, so we still have $w_{jt}^* = \xi_{jt} = W_{jt}^u$. Therefore, we have three active constraints $w_{jt} = \hat{w}_{jt}$ and $\hat{w}_{jt} = W_{jt}^e + w_{jt}^u - w_{jt}^l$, and $w_{jt}^l = 0$. Moreover, the active constraints $w_{jt}^u = W_{jt}^h$, and $w_{jt} = \xi_{jt}$ give the same limits and one of them is redundant. Our goal is to add the active constraint (10) to the master problem to ensure that when the first-stage decision changes, the scenario generated remains at the extreme point of the new set. To this end, here we remove the $w_{jt}^u = W_{jt}^h$.
- 2) If $\xi_{jt} = W_{jt}^l$ and $w_{jt}^* = W_{jt}^h$: Since $\hat{w}_{jt} = W_{jt}^e + w_{jt}^u - w_{jt}^l$ and $w_{jt}^u = W_{jt}^h$, we have $\hat{w}_{jt}^* = W_{jt}^l = \xi_{jt}$. Therefore, we have three active constraints $w_{jt} = \hat{w}_{jt}$, $\hat{w}_{jt} = W_{jt}^e + w_{jt}^u - w_{jt}^l$, and $w_{jt}^u = 0$. Moreover, the active constraints $w_{jt}^l = W_{jt}^h$ and $w_{jt} = \xi_{jt}$ give the same limits. For the reasons in 1), we remove the $w_{jt}^l = W_{jt}^h$.
- 3) If $\xi_{jt} = w_{jt}^e$ with $w_{jt}^* = w_{jt}^u = 0$: Since $\hat{w}_{jt} = W_{jt}^e + w_{jt}^u - w_{jt}^l$, we have $\hat{w}_{jt}^* = W_{jt}^e$. The two active constraints $w_{jt}^l = 0$ and $w_{jt}^u = 0$ gave the same limit as $w_{jt} = \xi_{jt}$. For the reasons in 1), we keep the $w_{jt} = \xi_{jt}$. For the constraint $w_{jt}^l = w_{jt}^u = 0$, due to the complementary condition $w_{jt}^l w_{jt}^u = 0$, we keep one of them and remove the other.

Dual degeneracy occurs if multiple solutions attain the optimal value, then the optimal solution is not unique. As in Fig. 1(b), a facet is perpendicular to the gradient of the objective function, so any point on the facet is an optimal solution. When there is dual degeneracy, the matrix $[H_{eq}, -C_{eq}]$ is not full-rank, and (10) is underdetermined. We can include some of the constraints in (11) to make $[H_{eq}, -C_{eq}]$ a full rank matrix, i.e., letting $H_{in,j}w = C_{in,j}\hat{w} + F_{in,j}\xi + G_{in,j}z^* + a_{in,j}$ for some j . If the unique w^* and \hat{w}^* we get satisfy constraint (11), then use the new set of constraints as the active constraint.

C. Master Problem

The master problem (MP) in iteration N is formulated as

$$\min_{x, \xi} c^\top x + g(\xi) + \eta \quad (13a)$$

$$\text{s.t. } x \in \mathbb{X}, \xi \in \Xi \quad (13b)$$

$$\eta \geq d^\top y^n, \forall n \in [N] \quad (13c)$$

$$H_{eq}^n \tilde{w}^n = C_{eq}^n \hat{w}^n + F_{eq}^n \xi + G_{eq}^n z^{n*} + a_{eq}^n, \forall n \in [N] \quad (13d)$$

$$w^n = \min\{\tilde{w}^n, \xi\}, w^n = \max\{W^l, \tilde{w}^n\}, \forall n \in [N] \quad (13e)$$

$$y^n \in \mathbb{F}(x, w^n), \forall n \in [N] \quad (13f)$$

The decision variables are $\{x, \xi, \eta, y^n, w^n, \tilde{w}^n, \hat{w}^n, \forall n \in [N]\}$. n is the index of scenarios. w^n is the RG output scenario in the n -th iteration while \tilde{w}^n and \hat{w}^n are intermediate variables. The constraints of the first-stage problem are given in (13b). Since η is minimized in the objective (13a), constraint (13c) is equivalent to $\eta = \max_n d^\top y^n$ which is the re-dispatch cost under the worst-case scenario. The constraints in the second-stage problem are given in (13f). Our key innovation lies in the scenario representation (13d)-(13e). Instead of adding the worst-case scenario in the previous iteration itself directly to the master problem as the traditional robust optimization methods [10], here we include the set of active constraints (13d). When the first-stage decision ξ changes, the \tilde{w}^n will change accordingly and can be uniquely determined by (13d). Together with (13e), we can ensure that the scenario w^n is still an extreme point of $\mathcal{W}(\xi)$. We will give an example to explain this in detail in the Remark later.

The constraint $w^n = \min\{\tilde{w}^n, \xi\}$ can be linearized as

$$\begin{aligned} W^l &\leq \tilde{w}^n \leq W^u, \quad z_w^n \in \{0, 1\}^{N_w \times T} \\ w^n &\leq \tilde{w}^n, \quad w^n \leq \xi \\ \tilde{w}^n - (W^u - W^l)z_w^n &\leq w^n \\ \xi - (W^u - W^l)(1 - z_w^n) &\leq w^n \end{aligned} \quad (14)$$

This is different from the linearization technique in (2) since now ξ is a variable instead of a constant. Constraint $w^n = \max\{W^l, \tilde{w}^n\}$ can be linearized in a similar way since it is equivalent to $-w^n = \min\{-W^l, -\tilde{w}^n\}$. The master problem MP is thus turned into a mixed-integer quadratic program (MIQP) that can be solved efficiently by commercial software.

Remark: Since $[H_{eq}^n, -C_{eq}^n]$ is a full-rank matrix, \tilde{w}^n and \hat{w}^n can be uniquely represented as a function of ξ . If \tilde{w}^n is a feasible point of the new $\mathcal{W}(\xi)$, then we have $\tilde{w}^n \leq \xi$ and $\tilde{w}^n \geq W^l$ due to the constraints in $\mathcal{W}(\xi)$. Therefore, $w^n = \tilde{w}^n$ is an extreme point of the new $\mathcal{W}(\xi)$. If \tilde{w}^n is infeasible for the new $\mathcal{W}(\xi)$, then constraint (13e) projects it onto an extreme point (vertex) of the new $\mathcal{W}(\xi)$. We use a simple example with two RGs for illustration:

Suppose $T = 1$ and the uncertainty set is ²

$$\mathcal{W}(\xi) = \left\{ (w_1, w_2)^\top \left| \begin{aligned} w_j &= \min\{\hat{w}_j, \xi_j\}, \forall j = 1, 2 \\ \hat{w}_j &= 4 + w_j^u - w_j^l, \forall j = 1, 2 \\ 0 &\leq w_j^u, w_j^l \leq 2, \forall j = 1, 2 \\ \frac{w_1^l + w_1^u}{2} + \frac{w_2^l + w_2^u}{2} &\leq \frac{3}{2} \end{aligned} \right. \right\} \quad (15)$$

Suppose in the $N - 1$ iteration, $\xi_1 = \xi_2 = 6$, so the feasible region is the grey region in Fig. 2(a). Suppose the optimal solution of the SP is point A. Primal degeneracy happens in this case and the constraints $w_2 \leq \xi_2$ and $w_2 \leq 6$ give the same

²The t index is omitted for simplicity.

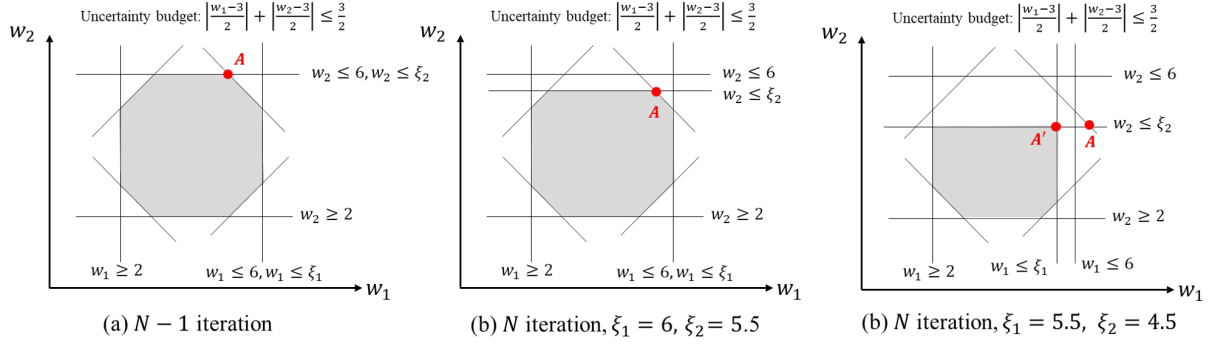


Fig. 2. Illustration of the adaptive RG power output scenario.

limit. According to Section III-B, we keep the former constraint and drop the latter one. Therefore, the scenario A can be represented as a function of ξ , i.e. $(\tilde{w}_1, \tilde{w}_2) = (11 - \xi_2, \xi_2)$. Then in the N iteration, if $\xi = (6, 5.5)$ as in Fig. 2(b), the active constraints remain unchanged. Substituting the value of ξ into the expression of point A , we can get a new point $A(\tilde{w}_1, \tilde{w}_2) = (5.5, 5.5)$, which is a vertex of the new $\mathcal{W}(\xi)$. If $\xi = (5.5, 4.5)$ as in Fig. 2(c), now the new point A is $(\tilde{w}_1, \tilde{w}_2) = (6.5, 4.5)$ which is outside of $\mathcal{W}(\xi)$. But with constraint (13e), the point $A(\tilde{w})$ is projected to point A' (w) which is again a vertex of the new set $\mathcal{W}(\xi)$.

D. Adaptive C&CG algorithm

The overall iterative algorithm is given in Algorithm 1.

Algorithm 1: : Adaptive C&CG Algorithm

- 1) **Initiation:** Error tolerance $\varepsilon > 0$; $N = 1$; Let $C_{eq}^N, F_{eq}^N, G_{eq}^N$ be zero matrices; Let H_{eq}^N be an identity matrix and $d_{eq}^N = W^e$.
 - 2) **Solve the Master Problem**
Solve the MP (13). Let (x^{N*}, ξ^{N*}) be the optimal solution and LB_N be the optimal value.
 - 3) **Solve the Subproblem**
Solve the SP (9) with (x^{N*}, ξ^{N*}) . Let $(w^{N*}, \hat{w}^{N*}, z^{N*}, y^{N*})$ be the optimal solution and $UB_N = c^\top x^{N*} + g(\xi^{N*}) + d^\top y^{N*}$.
 - 4) **Retrieve the active constraints**
Reduce redundant constraints (see Appendix A).
Deal with degenerate cases (see Section III-B).
Identify the set of active constraints \mathcal{AC}_N based on (10).
 - 5) if $|UB_N - LB_N| \leq \varepsilon$, terminate and output (x^{N*}, ξ^{N*}) .
Otherwise, $N = N + 1$, go to Step 2.
-

Theorem 1. The Algorithm 1 generates the optimal solution to problem (6) in finite iterations.

The proof of Theorem 1 can be found in Appendix B. The necessity and novelty of the proposed algorithm are highlighted below by comparing with two related algorithms.

- 1) **Nested C&CG** [24]. If we let \hat{w} be the variable of the middle “max” problem and move the constraint

$w = \min\{\hat{w}, \xi\}$ to the inner “min” problem. The problem obtained is equivalent to the original robust optimization model (6) while the new uncertainty set becomes decision-independent. The nonlinear constraint $w = \min\{\hat{w}, \xi\}$ in the inner “min” can be linearized as

$$w = \hat{w}z + \xi(1 - z) \\ w \leq \hat{w}, w \leq \xi, z \in \{0, 1\}^{N_w \times T} \quad (16)$$

Therefore, the problem is turned into a traditional robust optimization problem with integer variables in the second stage. Denote the optimal value of the inner “min” as $Q(x, \hat{w})$. Nested C&CG [24] might be applied to solve this problem. However, since $Q(x, \hat{w})$ is not quasiconvex in \hat{w} , there is no guarantee that the optimal solution of the “max-min” will reside at one extreme point (vertex) of the uncertainty set. Therefore, the algorithm may not terminate in finite steps. In case studies, we use nested C&CG for comparison. The results show that, apart from the convergence issue, our method can greatly reduce the computational time compared with nested C&CG.

- 2) **Modified Bender’s decomposition** [21]. The method in [21] deals with the robust optimization problem with a linear decision-dependent uncertainty set. Instead of adding the worst-case scenario to the master problem in each iteration, the corresponding dual variables are added with constraints to ensure that w will be the optimal solution of the inner “max-min” problem with the selected dual variable. This constraint is equivalently represented as the KKT condition of the middle “max” problem so that the master problem renders a mixed integer linear program. However, for the model in this paper, the uncertainty set is a mixed-integer linear set, and we cannot get its KKT condition.

IV. ILLUSTRATIVE EXPERIMENTS

We first use a IEEE-39 bus system with a single period for demonstration. Then a larger IEEE-118 bus system is tested to show the scalability and practicability of the proposed method. Detailed data can be found in [25].

A. IEEE-39 bus system

The IEEE-39 bus system has 10 thermal generators and 46 transmission lines. The parameters of the thermal generators

TABLE I
PARAMETERS OF THE THERMAL GENERATORS

Unit	P_i^l (MW)	P_i^u (MW)	R_i^\pm (MW)	α_i (\$/MW)	β_i^\pm (\$/MW)	d_i^\pm (\$/MW)
1	70	155	120	16.19	1.62	1.62
2	70	155	120	17.26	1.73	1.73
3	40	80	60	16.60	1.66	1.66
4	30	50	50	16.50	1.59	1.59
5	55	100	70	19.70	1.97	1.97
6	30	50	30	22.26	2.22	2.22
7	25	55	34	22.74	2.77	2.77
8	20	55	22	25.92	2.59	2.59
9	20	55	20	27.27	2.73	2.73
10	20	55	10	27.79	1.30	1.30

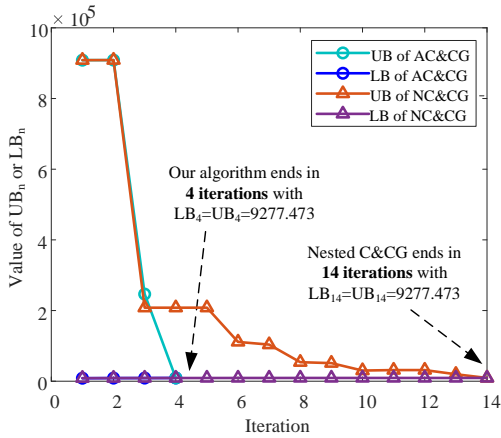


Fig. 3. Values of UB_N and LB_N during iterations.

are given in TABLE I. There are three RGs connected to the power grid at nodes 4, 14, 29, respectively. Their forecast outputs are $W^e = [150, 150, 150]^T$ MW and $W^l = 0.7W^e$, $W^u = 1.3W^e$. The uncertainty budget $\Gamma_S = 2$. The proposed Adaptive C&CG (AC&CG) algorithm and the Nested C&CG (NC&CG) algorithm are applied to solve the problem, respectively. The change of UB_N and LB_N during iterations are given in Fig. 3. We can find that both algorithms output the same solution with an optimal objective value of \$9,277.473 and the curtailment strategy $\xi = [176.45, 179.55, 164.09]^T$ MW. This verifies the proposed algorithm. The proposed AC&CG algorithm can greatly reduce the computational time since it only requires 4 iterations to reach the optimal solution whereas the NC&CG takes 14 iterations. Let alone the fact that in each iteration, the NC&CG algorithm takes another 3-4 iterations to solve the subproblem.

The decision-dependent uncertainty set in the 1st, 3rd, and 4th iterations are shown in Fig. 4. When the first-stage decision changes, the uncertainty set changes dramatically. As a result, a previously picked scenario, for example if it is point A, may fall outside of the uncertainty set. Continuing to use traditional robust optimization algorithms may result in over-conservative or infeasible results. This demonstrates the necessity of this work. The worst-case scenarios selected during the iterations of the two algorithms are plotted in Fig. 5 and Fig. 6, respectively. In each iteration, a different background color

represents a different set of active constraints.

In Fig. 5, the same set of active constraint recurs. For example, in the 7th to 13th iterations, the worst-case scenarios are generated by the same active constraint $w = \xi$. This is the root of the inefficiency of traditional algorithms: when the first-stage decision changes, the previously selected scenario may no longer be a vertex of the new uncertainty set. Therefore, there are an infinite number of possible uncertain scenarios and the algorithm does not necessarily stop in a finite number of steps. In contrast, in Fig. 6, the same set of active constraints appears only once. Instead of a fixed value, the previously selected scenario will change with the first-stage decision. The set of selected scenarios after the 2nd, 3rd, and 4th iterations are connected by the solid line, dashed line, and dash-dot line, respectively. For example, the scenario identified in the 2nd iteration is $w^{2*} = [195, 195, 150]^T$ MW, and thus, the active constraints are $w_1^2 = \xi_1$, $w_2^2 = \xi_2$, and $w_3^2 = w_2^1 + w_2^2 - 240$. In the 3rd iteration, it changes to $w_2^3 = [188.52, 189.6, 138.12]^T$ since the curtailment strategy changes to $\xi = [188.52, 189.6, 195]^T$ MW. Then as the curtailment strategy changes to $\xi = [176.45, 179.54, 164.09]^T$ MW in the 4th iteration, the scenario further changes to $w_2^4 = [176.45, 179.55, 116.00]^T$ MW.

B. IEEE-118 bus system: Benchmark

We further test the performance of our proposed algorithm using a larger IEEE-118 bus system. There are 54 thermal generators and 186 transmission lines. Our proposed algorithm (AC&CG) takes 4 iterations (17.53 seconds) to reach the robust optimal solution. The traditional nested C&CG takes 30 iterations (433.24 seconds). The change of UB_N and LB_N are given in Fig. 7. Since UB_N and LB_N vary in a wide range, therefore, we draw the $\log(UB_N)$ and $\log(LB_N)$ instead. Both algorithms output the same result while the proposed algorithm can greatly reduce the computational time.

The optimal curtailment strategy (ξ^*) as well as the upper/lower bound of the net load ($\sum_l D_{li} - \sum_i p_{li}$) and the RG power output ($\sum_j w_{ji}$) is shown in Fig. 8. With growing renewable energy penetration, in many periods (e.g., 1-19h), the upper bound of the total RG power output is higher than the upper bound of the net load, i.e., $W^u > \sum_l D_{li} - \sum_i p_{li}^u$. Therefore, curtailment is required; and correspondingly, the red curve in Fig. 8 is lower than the upper grey curve (W^u). In hours 20 and 21, the maximum net load is higher than the maximum RG power output, and thus, there is no curtailment. However, in hour 22, even though the maximum net load is higher than the maximum RG power output, curtailment still occurs, which is caused by the ramping capacity limit. From Fig. 8 we can find that, curtailment happens in most of the time, and if all are done in real-time without a preparatory schedule, it will result in frequent emergency controls that will jeopardize the system's stability. That's why we need to decide on the curtailment schedule in the pre-dispatch stage.

Four typical scenarios are selected from the uncertainty set in the last iteration of the nested C&CG algorithm and the proposed algorithm, respectively. They are plotted in Fig. 9 together with the optimal curtailment strategy. When applying

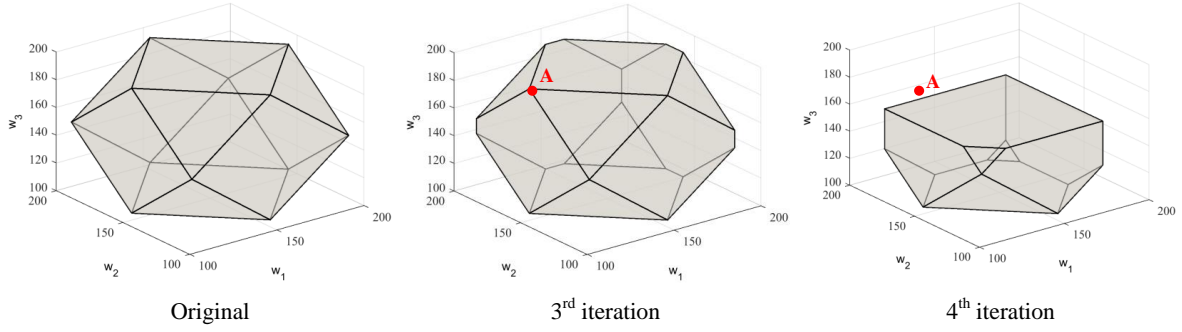


Fig. 4. Decision-dependent uncertainty sets.

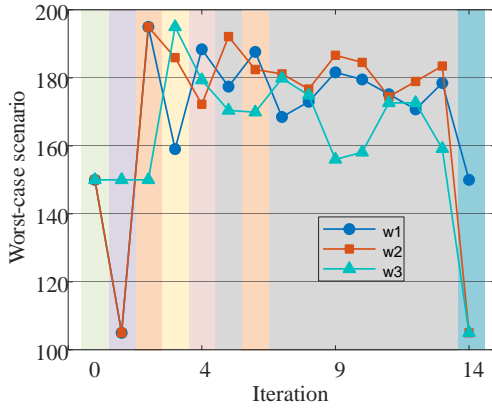


Fig. 5. Worst-case scenarios during iterations of the nested C&CG.

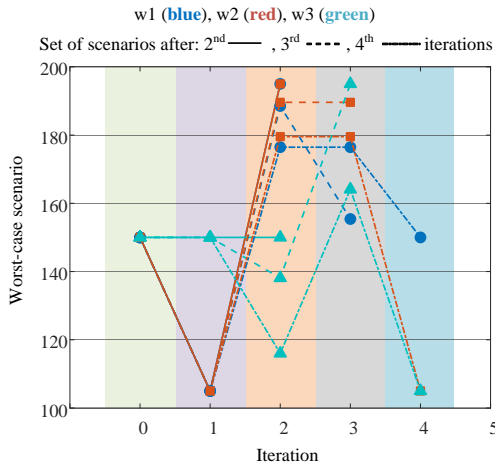


Fig. 6. Worst-case scenarios during iterations of our proposed algorithm.

the nested C&CG algorithm, we move the $w = \min\{\hat{w}, \xi\}$ constraint to the inner “min” problem and turn the uncertainty set into a decision-independent one, which is the shaded area in Fig. 9(a) (for more details, please refer to Section III-D). First, we can find that scenarios 2 and 4 exceed the upper limit imposed by the curtailment strategy. Thus, they are not feasible for the original decision-dependent uncertainty set (1) and this makes the traditional C&CG not applicable. Moreover, the selected scenarios (e.g. scenarios 1 and 3) may not be vertices of the decision-dependent uncertainty set (shaded

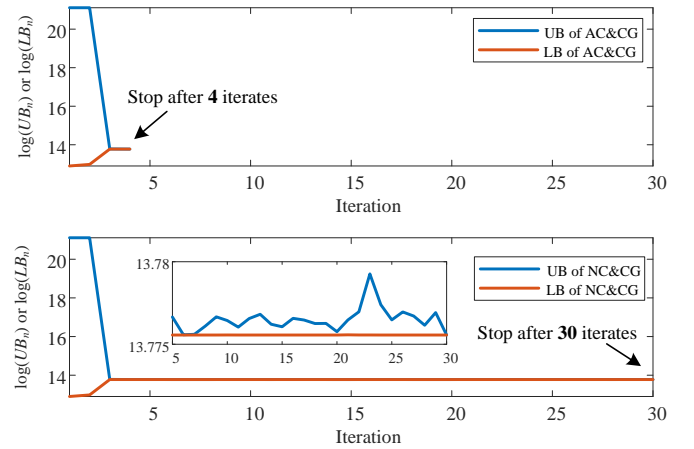
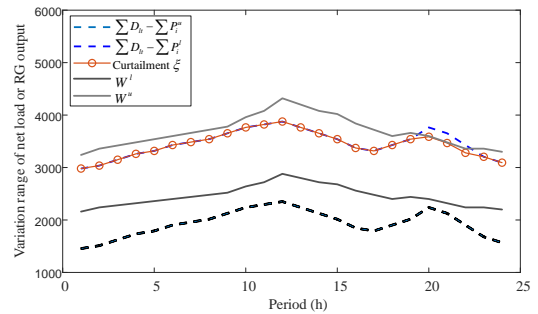
Fig. 7. Values of $\log(UB_N)$ and $\log(LB_N)$ during iterations.

Fig. 8. Curtailment strategy and variation range of net load and RG output.

area). Therefore, there is no guarantee that the nested C&CG algorithm will stop after a finite number of iterations. In contrast, under the proposed algorithm, the previously selected algorithm can change adaptively and all remains feasible for the new uncertainty set as in Fig. 9(b).

C. IEEE-118 bus system: Impact of different factors

In the following, we analyze the impact of several factors. First, we change the ramping limit $\mathcal{R}_i^u, \mathcal{R}_i^d, \forall i$ from 1.0 to 3.0 times of their original values. The results are shown in TABLE II. Originally, when the ramping limits are small, curtailment will be needed even if the maximum net load exceeds the

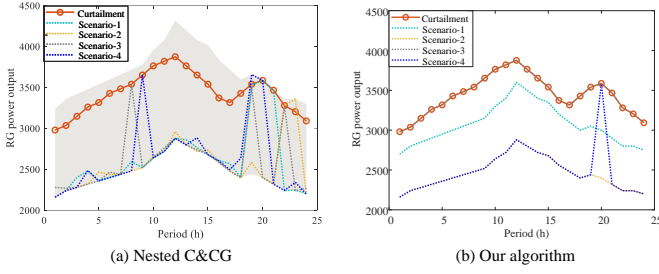


Fig. 9. Selected worst-case scenarios under two algorithms.

TABLE II
COSTS AND TIMES UNDER DIFFERENT RAMPING LIMITS

Ratio	Curtailment cost (\$)	Total cost (\$)	Time (s)
1.0	505,793.39	960,836.16	17.53
1.3	504,915.80	943,105.19	35.03
1.5	504,833.43	937,835.58	43.52
2.0	504,789.02	932,740.06	61.14
2.5	504,789.02	932,034.86	62.61
3.0	504,789.02	932,034.86	60.68

maximum RG output, similar to Fig. 8. As the limits enlarge, we are able to set the curtailment to the maximum net load. Therefore, the curtailment cost first decreases dramatically and then remains unchanged. When the ratio changes from 2.0 to 2.5, even though the curtailment costs are the same, the total cost declines. This is because larger ramping limits enable a better allocation of contemporary output and reserve capacity of thermal units. Then, when the ratio changes from 2.5 to 3.0, both the curtailment cost and total cost remain unchanged since ramping limits are no longer binding factors. Moreover, the computational times are all acceptable.

Furthermore, we test the performance of the two algorithms under different levels of uncertainty as given in TABLE III. When the uncertainty decreases, both the curtailment cost and the total cost decline, which is straightforward. With higher uncertainty, the number of iterations needed by the proposed AC&CG algorithm is stable while that taken by the NC&CG is less predictable. This shows the superiority of the proposed algorithm in the future power system with severe renewable energy fluctuations.

V. CONCLUSION

In this paper, a novel RGD model considering preparatory schedule of renewable power curtailment is proposed. The model casts down to a robust optimization with DDU. An adaptive C&CG algorithm was developed to solve the problem efficiently by identifying the active constraints in each iteration and adding them to the master problem. In this way, the worst-case scenarios remain to be vertices of the uncertainty set when the first-stage decision changes. Our main findings are:

1) We prove theoretically that the proposed algorithm can generate the robust optimal solution in a finite number of iterations. Many of the existing algorithms do not have this guarantee due to the decision-dependent uncertainty.

TABLE III
COSTS AND TIMES UNDER DIFFERENT UNCERTAINTY LEVELS

$[W^l, W^u]$	Curtailment cost (\$)	Total cost (\$)	No. of iterates AC&CG / NC&CG
$[0.80, 1.20]W^e$	505,793.39	960,836.16	4 / 30
$[0.85, 1.15]W^e$	156,837.81	591,204.55	4 / 10
$[0.90, 1.10]W^e$	21,616.34	439,438.98	4 / 5
$[0.95, 1.05]W^e$	45.97	407,812.56	3 / 4
$[1.00, 1.00]W^e$	0.00	399,610.92	1 / 1

2) The proposed algorithm can reduce the computational time by 95% compared with the nested C&CG algorithm.

3) With higher uncertainty, the performance of the proposed algorithm remains stable while the number of iterations needed by the nested C&CG is less predictable.

APPENDIX

A. Redundancy Elimination

A redundant constraint in $\mathcal{W}(\xi)$ is defined as follows.

Definition A1. (Redundant Constraint) Given ξ and z^* , a constraint is *redundant* if removing that constraint does not change the uncertainty set $\mathcal{W}(\xi)$.

Denote $Q := [H, -C]$, $u := [w^\top, \hat{w}^\top]^\top$, and $q := F\xi + Gz^* + a$. Then the redundant constraints can be removed with the help of the following theorem.

Theorem A1. Constraint $Q_j u \leq q_j$ is redundant if the following linear programming has a feasible solution

$$v^\top Q_{[-j]} = Q_j, \quad q_j \geq v^\top q_{[-j]}, \quad v \geq 0 \quad (\text{A.1})$$

Proof. If constraint $Q_j u \leq q_j$ is redundant, the polytope $\{u | Q_{[-j]} u \leq q_{[-j]}\}$ defined by the remaining constraints must be a subset of $\{u | Q_j u \leq q_j\}$. Therefore, we have $\{u | Q_{[-j]} u \leq q_{[-j]}\} \cap \{u | Q_j u > q_j\} = \emptyset$. According to the Nonhomogeneous Farkas Lemma [26], it is equivalent to the set \mathcal{Q} defined below is non-empty.

$$\mathcal{Q} = \{v | v^\top Q_{[-j]} = Q_j, \quad q_j \geq v^\top q_{[-j]}, \quad v \geq 0\} \quad (\text{A.2})$$

In other words, the corresponding linear programming has a feasible solution. \square

By checking each of the constraints in $\mathcal{W}(\xi)$, remove the redundant ones, and identify the active constraints, we can avoid the primal degeneracy.

B. Proof of Theorem 1

We start the proof of Theorem 1 with the following lemma.

Lemma B1. Suppose the optimal solution of (6) is (x^*, ξ^*) . Let N be the iteration run of Algorithm 1. For any $n \in [N]$:

- $LB_n \leq c^\top x^* + g(\xi^*) + S(x^*, \xi^*) \leq UB_n$
- For any $n_1, n_2 \in [N-1]$, the set of active constraints \mathcal{AC}_{n_1} won't be the same as the set of active constraints \mathcal{AC}_{n_2} .
- If there exists some $n \in [N-1]$ whose set of active constraints \mathcal{AC}_n is the same as \mathcal{AC}_N , the algorithm terminates in N .

Proof. Assertion (a): For each $n \in [N]$, constraints (13d) and (13e) give a feasible point of $\mathcal{W}(\xi)$. The robust optimization problem (6) can be equivalently written as

$$\min_{x, \xi} c^\top x + g(\xi) + \eta \quad (\text{B.1a})$$

$$\text{s.t. } x \in \mathbb{X}, \xi \in \Xi \quad (\text{B.1b})$$

$$\eta \geq Q(x, w), \forall w \in \mathcal{W}(\xi) \quad (\text{B.1c})$$

while the master problem **MP** is

$$\min_{x, \xi} c^\top x + g(\xi) + \eta \quad (\text{B.2a})$$

$$\text{s.t. } x \in \mathbb{X}, \xi \in \Xi \quad (\text{B.2b})$$

$$\eta \geq Q(x, w), \forall w \in \Gamma(\text{Sol}(\mathcal{AC}_n, \xi)) \quad (\text{B.2c})$$

where $\text{Sol}(\mathcal{AC}_n, \xi)$ refers to the unique solution of the set of active constraints \mathcal{AC}_n given ξ and $\Gamma(\cdot)$ refers to the projection exerted by (13e). Then, w^n is a feasible point of $\mathcal{W}(\xi)$. The two problems (B.1) and (B.2) have the same objective functions while the constraint (B.2c) is a relaxation of (B.1c). Therefore, the optimal value of (B.2), i.e., LB_n , is no more than that of (B.1), i.e., $c^\top x^* + g(\xi^*) + S(x^*, \xi^*)$. Moreover, we have $UB_n = c^\top x^{n*} + g(\xi^{n*}) + S(x^{n*}, \xi^{n*})$. Due to the optimality of (x^*, ξ^*) , we have $UB_n \geq c^\top x^* + g(\xi^*) + S(x^*, \xi^*)$.

Assertion (b): If we have \mathcal{AC}_{n_1} be the same as \mathcal{AC}_{n_2} . Then, $w^{n_2*} = \Gamma(\text{Sol}(\mathcal{AC}_{n_2}, \xi^{n_2*})) = \Gamma(\text{Sol}(\mathcal{AC}_{n_1}, \xi^{n_2*}))$. We have $UB_{n_2} = c^\top x^{n_2*} + g(\xi^{n_2*}) + Q(x^{n_2*}, w^{n_2*})$. Moreover, η in the master problem is the maximum of $Q(x^{n_2*}, w)$ for all $w \in \Gamma(\text{Sol}(\mathcal{AC}_j, \xi^{n_2*}))$, $j = [n_2 - 1]$. so $\eta \geq Q(x^{n_2*}, w^{n_1*}) = Q(x^{n_2*}, w^{n_2*})$. Therefore, $LB_{n_2} \geq UB_{n_2}$. Together with $UB_{n_2} \geq LB_{n_2}$, we have $LB_{n_2} = UB_{n_2}$, and the algorithm terminates in the n_2 iteration, which is contradict to the fact that $N > n_2$ is the iteration run.

Assertion (c): Following a similar procedure as in the proof of (b), it is easy to get (c). \square

Now the proof of **Theorem 1** is given below.

First, we prove that the algorithm terminates in a finite number of iterations. According to Lemma B1(b)-(c), the same set of active constraints won't be attached twice. Moreover, each set of active constraints is composed of $4N_w \times T$ linearly-independent constraints from $\mathcal{W}(\xi)$. Since there are a finite number of those possible combination of constraints, the algorithm will terminate in finite steps.

Next, we show the optimality of (x^{N*}, ξ^{N*}) . According to Lemma B1(a), we have $LB_N \leq c^\top x^* + g(\xi^*) + S(x^*, \xi^*) \leq UB_N$. Together with the condition for termination $|UB_N - LB_N| \leq \varepsilon$. Therefore,

$$\begin{aligned} & |c^\top x^N + g(\xi^N) + S(x^N, \xi^N) - (c^\top x^* + g(\xi^*) + S(x^*, \xi^*))| \\ &= |UB_N - (c^\top x^* + g(\xi^*) + S(x^*, \xi^*))| \\ &\leq |UB_N - LB_N| \leq \varepsilon \end{aligned} \quad (\text{B.3})$$

which justifies the optimality of (x^{N*}, ξ^{N*}) . \square

REFERENCES

- [1] G. W. E. Council, "GWEC-global wind report 2021," *Global Wind Energy Council: Brussels, Belgium*, 2021.
- [2] M. Schmela, W. Hemetsberger, and G. Chianetta, "Global market outlook for solar power 2021–2025," *SolarPower Europe, July*, 2021.
- [3] W. Wei, F. Liu, S. Mei, and Y. Hou, "Robust energy and reserve dispatch under variable renewable generation," *IEEE Transactions on Smart Grid*, vol. 6, no. 1, pp. 369–380, 2014.
- [4] Y. Fu, M. Liu, and L. Li, "Multiobjective stochastic economic dispatch with variable wind generation using scenario-based decomposition and asynchronous block iteration," *IEEE Transactions on Sustainable Energy*, vol. 7, no. 1, pp. 139–149, 2015.
- [5] Z. Hu, Y. Xu, M. Korkali, X. Chen, L. Mili, and J. Valinejad, "A Bayesian approach for estimating uncertainty in stochastic economic dispatch considering wind power penetration," *IEEE Transactions on Sustainable Energy*, vol. 12, no. 1, pp. 671–681, 2020.
- [6] A. Lorca and X. A. Sun, "Adaptive robust optimization with dynamic uncertainty sets for multi-period economic dispatch under significant wind," *IEEE Transactions on Power Systems*, vol. 30, no. 4, pp. 1702–1713, 2014.
- [7] Y. Chen, W. Wei, F. Liu, and S. Mei, "Distributionally robust hydro-thermal-wind economic dispatch," *Applied Energy*, vol. 173, pp. 511–519, 2016.
- [8] W. Wei, F. Liu, and S. Mei, "Distributionally robust co-optimization of energy and reserve dispatch," *IEEE Transactions on Sustainable Energy*, vol. 7, no. 1, pp. 289–300, 2015.
- [9] D. Bertsimas, E. Litvinov, X. A. Sun, J. Zhao, and T. Zheng, "Adaptive robust optimization for the security constrained unit commitment problem," *IEEE transactions on power systems*, vol. 28, no. 1, pp. 52–63, 2012.
- [10] B. Zeng and L. Zhao, "Solving two-stage robust optimization problems using a column-and-constraint generation method," *Operations Research Letters*, vol. 41, no. 5, pp. 457–461, 2013.
- [11] S. Liu, Z. Bie, J. Lin, and X. Wang, "Curtailement of renewable energy in northwest China and market-based solutions," *Energy policy*, vol. 123, pp. 494–502, 2018.
- [12] Z. Wu, P. Zeng, X.-P. Zhang, and Q. Zhou, "A solution to the chance-constrained two-stage stochastic program for unit commitment with wind energy integration," *IEEE Transactions on Power Systems*, vol. 31, no. 6, pp. 4185–4196, 2016.
- [13] G. Morales-España, Á. Lorca, and M. M. de Weerd, "Robust unit commitment with dispatchable wind power," *Electric Power Systems Research*, vol. 155, pp. 58–66, 2018.
- [14] Y. Yang, W. Wu, B. Wang, and M. Li, "Chance-constrained economic dispatch considering curtailment strategy of renewable energy," *IEEE Transactions on Power Systems*, vol. 36, no. 6, pp. 5792–5802, 2021.
- [15] W. Yin, Y. Xue, S. Lei, and Y. Hou, "Multi-stage stochastic planning of wind generation considering decision-dependent uncertainty in wind power curve," in *2019 IEEE PES Innovative Smart Grid Technologies Europe (ISGT-Europe)*. IEEE, 2019, pp. 1–5.
- [16] B. Tarhan, I. E. Grossmann, and V. Goel, "Stochastic programming approach for the planning of offshore oil or gas field infrastructure under decision-dependent uncertainty," *Industrial & Engineering Chemistry Research*, vol. 48, no. 6, pp. 3078–3097, 2009.
- [17] O. Nohadani and K. Sharma, "Optimization under decision-dependent uncertainty," *SIAM Journal on Optimization*, vol. 28, no. 2, pp. 1773–1795, 2018.
- [18] N. H. Lappas and C. E. Gounaris, "Robust optimization for decision-making under endogenous uncertainty," *Computers & Chemical Engineering*, vol. 111, pp. 252–266, 2018.
- [19] P. Vayanos, A. Georghiou, and H. Yu, "Robust optimization with decision-dependent information discovery," *arXiv preprint arXiv:2004.08490*, 2020.
- [20] S. Avraamidou and E. N. Pistikopoulos, "Adjustable robust optimization through multi-parametric programming," *Optimization Letters*, vol. 14, no. 4, pp. 873–887, 2020.
- [21] Y. Zhang, F. Liu, Z. Wang, Y. Su, W. Wang, and S. Feng, "Robust scheduling of virtual power plant under exogenous and endogenous uncertainties," *IEEE Transactions on Power Systems*, 2021.
- [22] J. Fortuny-Amat and B. McCarl, "A representation and economic interpretation of a two-level programming problem," *Journal of the operational Research Society*, vol. 32, no. 9, pp. 783–792, 1981.
- [23] R. T. Rockafellar, *Convex analysis*. Princeton university press, 2015.
- [24] L. Zhao and B. Zeng, "An exact algorithm for two-stage robust optimization with mixed integer recourse problems," *submitted, available on Optimization-Online. org*, 2012.
- [25] [Online] Available: <https://sites.google.com/site/yuechenthul/data-sheet>.
- [26] Z. Xu, "Generalization of nonhomogeneous Farkas' Lemma and applications," *Journal of Mathematical Analysis and Applications*, vol. 186, no. 3, pp. 726–734, 1994.